Radiocarbon, Vol 59, Nr 3, 2017, p 957–965 DOI:10.1017/RDC.2016.38
Selected Papers from the 2015 Radiocarbon Conference, Dakar, Senegal, 16–20 November 2015

INCREASED ^{14}C AMS EFFICIENCY FROM REDUCED COMPETITIVE IONIZATION

John S Vogel[1*] • Jason A Giacomo[2]

[1]University of California (retired); 8300 Feliz Creek Dr., Ukiah, CA 95482, USA.
[2]Eckert Ziegler AG/Vitalea Science; 2121 Second St., Davis, CA 95618, USA.

ABSTRACT. Observation of 80 μA/mm^2 C^- current from a 0.5-mm-diameter sample compared to 20 μA/mm^2 from a 1-mm-diameter sample contradicts the long-held surface ionization hypothesis of cesium sputter ion source operation. Resonant ionization occurs in neutral Cs plasma above a sample in a sputtered pit or well. A collision-radiation model of that plasma followed electronic excitation and radiation relaxation up to the Cs(7d) state. The Cs(5d) metastable state dominates plasma in a 1-mm-diameter well, but high electron densities in narrow wells drive a majority to Cs(7d) and higher. Competitive ionization by Al_2 dimers from the sample holder reduces Cs(7s,p) states resonant in ionization energy with C^-. Al anions from states above Cs(7p) in narrow wells also diminish radiation cascades to the Cs(7s,p), reducing C^-. We tested sample wells of non-ionizing Zn to maintain high ionization efficiency for small samples in narrow wells.

KEYWORDS: AMS, carbon, cesium, anion, ionization.

INTRODUCTION

A theory of electron-capture ionization in cesium sputter ion sources (CSIS) arose 30 years ago based on the quantum tunneling mechanisms that describe negative secondary-ion mass spectrometry (SIMS) (Nørskov and Lundqvist 1979; Litherland et al. 1987; Gnaser 2008). This theory predicts <3% of the sputtered carbon to be anions (Litherland et al. 1987) and offers no predictive value in improving ion sources other than to cool the sample for maintaining Cs on the sample. Such cooling has proven ineffective in over 35 years of ion source development. Demonstration of 35% ionization efficiency in reaching C^- beams of >300 μA shows that a much more efficient physical process is at work in most CSIS used in accelerator mass spectrometry (AMS) for ^{14}C measurements (Fallon et al. 2007). The recent report of a 80 μA/mm^2 C^- current density from a 0.5-mm ⌀ (diameter) sample compared to 20 μA/mm^2 from 1-mm ⌀ confirms that anion production does not scale as surface area (Shanks and Freeman 2015). This example shows an equal C^- current from a 1-mm ⌀ sample well in an aluminum holder as from a sample in a 0.5-mm-diameter well that had 0.25-mm-thick iron coat over the aluminum walls of the sample recess. In this paper, we explain this effect in light of competitive ionization for resonant electron transfer.

We questioned surface anion production for CSIS when we found that the AMS at Vitalea Science is capable of making absolute isotope ratio measurements of a NIST ^{14}C standard, OxII SRM--4990c, for over a year to within 0.22 ± 0.06% from 577 measures (Vogel et al. 2013). Ockham's razor requires that every part, including the CSIS, also operate at low fractionation. Surface ionization predicts significant isotope fractionation (>6%) due to surface details and the different velocities of isotopes (Williams 1979; Litherland et al. 1987). Our observed low fractionation does not deny the nearly universally seen fractionation in other ion sources, but prompted a study of alternative ionization. The appearance of a blue plasma due to Cs^0(7p) relaxation above samples in AMS CSIS, in conjunction with maximum CSIS anion production during plasma appearance, suggests that ionization occurs in the plasma, separate from sputtering (Middleton et al. 1994; Middleton and Klein 1999). However, electron transfer between neutral atoms in a low-energy plasma of Cs vapor is incompatible with collision energetics of atomic ground states. Vora et al. (1974) show Cs^0(6p) transfers electrons to oxygen atoms at lower energies with increased probability in a resonant electron transfer (RET) model of ion-pair production.

*Corresponding author. Email: johnsvogel@yahoo.com.

Resonant electron transfer, producing ion pairs from colliding neutral atoms, was first described by Lee and Mahan (1965) to explain photoionization of alkali metal vapor at energies below the ionization potential (IP). They determined minimum values for electron affinity (EA) of the alkali atoms and minimum binding energies for alkali dimer ions. This method of finding electron affinities became standard practice (Nalley and Compton 1971), and is reviewed for atoms, ions, and molecules by Kleyn and Moutinho (2001). Barbier et al. (1986) show that thermal collisions of neutral alkali atoms give ion pairs when the ionization energy of a photoexcited state approaches the electron affinity. Narits et al. (2014) demonstrate the theory and present calculations of ion-pair production cross-sections from neutral collisions of Rydberg alkali atoms on alkali-earth atoms at ground state. Ion-pair production is most dependent on the anion binding energy and the "crossing radius," R_c, at which the ion-pair potentials cross the covalent potential energy curve of the collision quasimolecule. Figure 1 shows putative potential energy curves for the C^0 on Cs^0 collision with the Cs^0 in its ground and 4 excited states. The covalent curves are notional and repulsive for a nonexistent CsC quasimolecule (cesium carbide is Cs_2C_2). Curve crossings only occur when the ionic energy matches that of a Cs excited state. Maximum cross-sections for ion-pair production are approximated in Landau-Zener (LZ) theory as $1.42 \bullet R_c^2$. Elements with low EA have large R_c and high probabilities of pair production due to the large radius of the anion electron wave function coupling to the large radius of a resonant Rydberg electron. The ion-pair cross-sections for C^0 on Cs^0 in Figure 1 range from $40 Å^2$ for the Cs(6s) ground state to over $2500 Å^2$ for the Cs(7s) state.

We developed a collision-radiation model of the Cs plasma to find the relative densities of states in mm-sized cylindrical voids receiving mA Cs^+ primary beams (Vogel 2013). The model

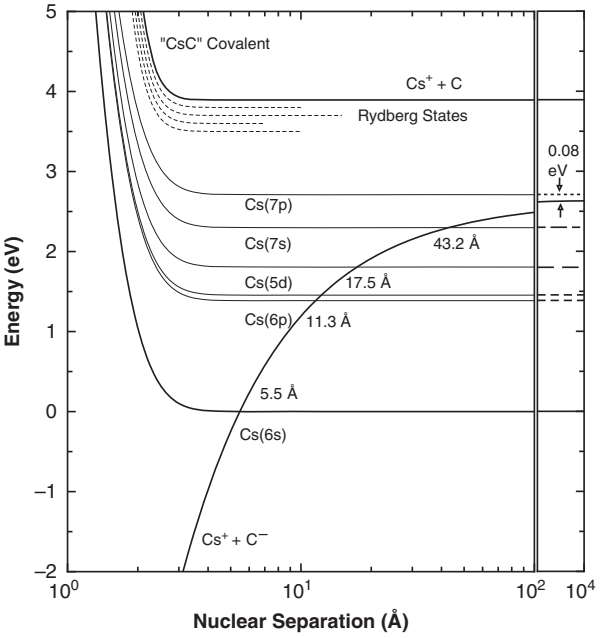

Figure 1 Born-Oppenheimer plot of the covalent and ionic potential energy curves for a C on Cs collision show crossings at radii, R_c, when the ionic energy equals the energy of Cs excited states. Collisional cross-sections to the ion pair are approximately $1.44\ R_c^2$.

https://doi.org/10.1017/RDC.2016.38 Published online by Cambridge University Press

is inspired by Norcross and Stone (1968) but is limited in scope, yielding only the densities of low-lying states. The model shows that the density of Cs above a recessed C sample reaches 10^{12}–10^{14} Cs/cm^3, optically thick for the Cs(6s)–Cs(6p) resonant infrared radiation. Secondary sputtered electrons maximizing at ≈2eV in Boltzmann distributions are capable of exciting Cs (6p) to successively higher excited states. We modeled state quantities up to Cs(7d), with the available electron excitation cross-sections of Krishnan and Stumpf (1992). Results for the Cs(7d) state are the sum for that and higher states, since the cross-sections are large for further low-energy excitations [e.g. 10^5Å^2 for Cs(8p) to Cs(7d)]. A 1-mm ⌀ sample well has a maximum population at Cs(5d), a metastable state with lifetime of 1.25 μs. Narrowing the sample well to 0.5 mm drives a majority to Cs(7d) and higher by increasing the density of the secondary sputtered electrons (Vogel 2016). Electron collisions occur with a 38-MHz rate at the assumed plasma temperature and densities (Bullis and Flavin 1964), much higher than the 3.5-Mhz decay of the Cs(7p). The Cs(7s,p) states in near resonance with the EA of carbon are created by both electron excitation from Cs(5d) and by radiative relaxation from higher states. Marcum et al. (1991) find that 30% of the Cs(7p) population in an electron excitation cell arises from radiation cascade from higher states. The RET mechanism for carbon on cesium is outlined in Figure 2. The emittance lines of Cs(7p) at 455 and 459 nm are the source of the blue color of the plasma. If a 0.5-mA beam of primary Cs^+ sputtered 5 C atoms per ion into a Cs^0(7s,p) cloud of 10^{11}Cs/cm^3 with a pair production cross-section of 2500 Å^2, a C^- current of 60 μA per mm of plasma is predicted.

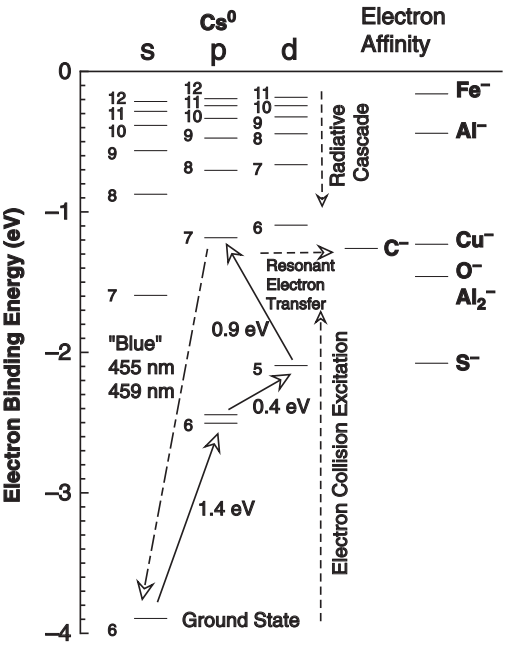

Figure 2 Ionization potentials of Cs excited states are compared to the electron affinities of carbon and other elements. A collision-radiation model of Cs vapor shows that electron collision excitement drives Cs to higher states while a radiation cascade lowers the states. Blue plasma in sputter ion sources reveals the Cs(7p) state.

https://doi.org/10.1017/RDC.2016.38 Published online by Cambridge University Press

Figure 2 shows other elements have EA near resonance with Cs(7s,p), particularly Cu at 1.228 eV. Cu sample holders were used when sample temperature was thought important (Middleton 1989), but early AMS development showed that Al sample holders gave twice the C^- ion current. Sputtered Cu^0 atoms are in direct competition with C^0 for capturing the Cs(7s,p) electrons and halve the C^- ionization. Shanks and Freeman (2015) confirm this halving of current by Cu. Such "competitive" ionization explains many mysteries of ion "sorcery" of the last 3 decades. For example, sulfur at low concentrations is known to "poison" a CSIS for most other elements. Figure 2 shows that S^- has an EA only 0.007 eV different from the IP of $Cs(5d_{5/2})$, giving it an enormous pair-production cross-section. Sulfur removes the Cs(5d) target atoms for exciting Cs to Cs(7p) and higher. Sulfur's high probability of ionization from the copious Cs(5d) makes even slight traces of ^{36}S in ^{36}Cl AMS samples into serious background that can be reduced by adding iridium to the sample (Vogel 2015). Middleton (1989) shows the aluminum dimer dominates sputtering from that metal. With an EA equivalent to oxygen's (1.46 eV), Al_2 and O are also strong competitors for Cs(7s) with C and can block excitations from Cs(5d). O^- likely reduces the C^- output of CO_2 ion sources. These sources could use laser photoexcitation at 455.5 nm to excite Cs^0 directly to Cs (7p) without passing through the Cs(5d) state by electron excitation. C^- should also increase if CO were used instead of CO_2.

Shanks and Freeman (2015) demonstrate that small C samples, recessed in 0.5-mm ⌀ wells having Fe-coated walls, produce as much C^- current as larger samples in 1-mm ⌀ wells in Al holders. We attribute this to competitive ionization for Cs(7s) by sputtered Al_2 and by Al ionizing states above Cs(7p), reducing its production from cascade radiation, as indicated in Figure 2 (Vogel 2015). Fe-coated walls eliminate this competitive ionization from both Al and Al_2. Sputtered Fe could also reduce C^- if electron excitation promoted cesium to Cs(12p, 11d). The lack of effect shows that electron excitation does not extend to those levels in their CSIS. We hypothesized that sample holders of a metal that cannot form an anion would minimize losses from competitive ionization. The only metals fitting this requirement in the main periodic table are reactive magnesium, liquid mercury, toxic cadmium, plus the likely candidates of manganese and zinc. We replaced the Al surrounding the sample well with zinc, chosen for its availability in high purity at low cost in many physical forms.

METHODS

Sample holders were modified as shown in Figure 3. Holes were drilled and reamed to 3.15-mm (0.124 in.) diameter at a 5 mm depth in the front of the Al holders. Zn wire of 0.125-in. diameter (Alfa Aesar #10435, Ward Hill, MA) was cut to 7-mm lengths. Al slugs of the same diameter (Alfa Aesar #42258) acted as controls. The metal slugs were press-fit (hammered) into the holes for a tight, thermal fit. The excess insert metal was machined off, and a 118° countersink made a funnel/lens. Sample holes were drilled to a depth of 1.5 mm at ⌀ of 0.5, 0.6, 0.7, 0.8, 1.0, and 1.25 mm. Fullerene soot (Alfa Aesar #50971) mixed with -325 mesh iron powder (Sigma-Aldrich #209309, St. Louis, MO, USA) at a weight ratio of approximately 1:10 were samples. Three sample wells for each insert type and well diameter were filled to approximately 1 mm of the top (36 in all). Samples were tamped into place only by finger pressure with a drill stem. The CSIS was operated at 8-kV cathode potential drawing 1–2 mA current. The samples were measured in rotation, with a Zn holder following an Al holder of the same well diameter for three cycles, spending 6.5 min on each sample for each cycle. Ion currents were quantified for $^{12}C^-$ and $^{12}C^+$ in a MICADAS AMS.

https://doi.org/10.1017/RDC.2016.38 Published online by Cambridge University Press

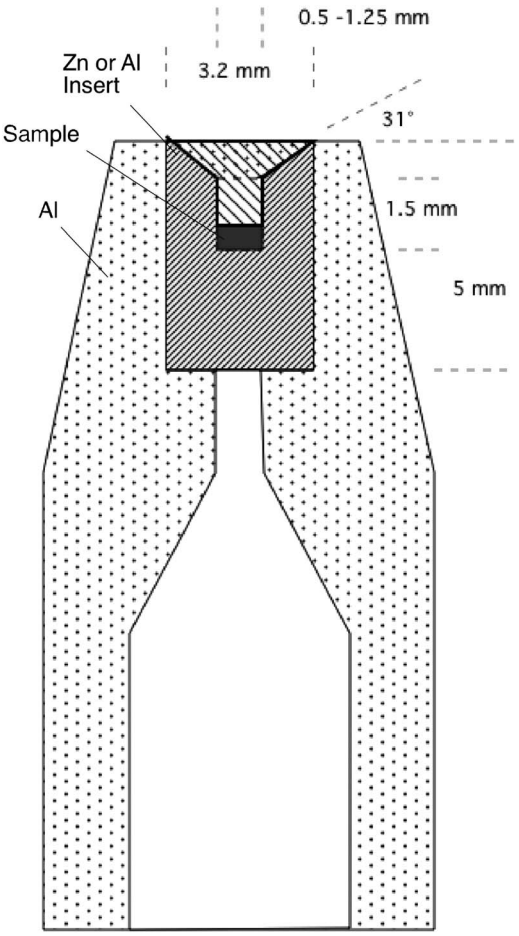

Figure 3 MICADAS sample holders were modified by cylindrical metal inserts into which sample holes were drilled to a depth of 1.5 mm with diameters of 0.5, 0.6, 0.7, 0.8, 1.0, and 1.25 mm.

RESULTS

Figure 4 shows a Zn-INSERT sample holder with a 0.5-mm-diameter well after the 20-min sputtering. The edges of the sample well show little erosion. Primary Cs^+ appears to be focused 2 mm behind the front of the sample holder, making a sputter "shadow" of ≈1.6 mm on the metal insert. The "rolled" appearance at the edges of the Zn insert is due to the countersink operation and is not melted Zn, although melting could be a concern in a more intense CSIS.

Figure 5a shows the $^{12}C^-$ ion current of the samples as functions of well ⌀ for both Al and Zn inserts. No significant differences were found for the 1- and 1.25-mm well diameters within the large error bars for both metals. Large uncertainties perhaps arose from the gentle pressure used in securing the sample, but it is unclear why variations were greater for Zn than Al. The narrow wells in Zn produced 25% higher currents than the 1-mm well in Al. The line fit to the Zn data is derived from area integrals of a Gaussian-shaped Cs^+ beam striking the sample, as shown in Figure 6. The Al data was fit by subtracting from this the integrals of Gaussian "rings" striking the Al metal,

https://doi.org/10.1017/RDC.2016.38 Published online by Cambridge University Press

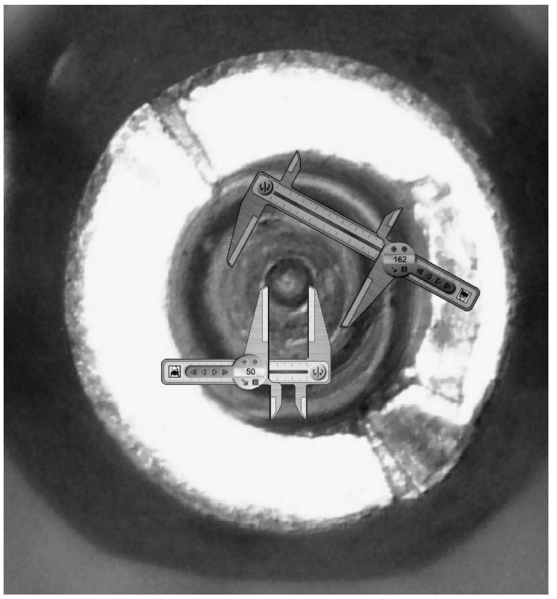

Figure 4 The front of a sample holder is shown with a Zn insert and a 0.5-mm sample well. A focus point (⌀ ≈ 0.1 mm) is seen at the bottom of the well and the erosion mark around the well is approximately 1.62 mm.

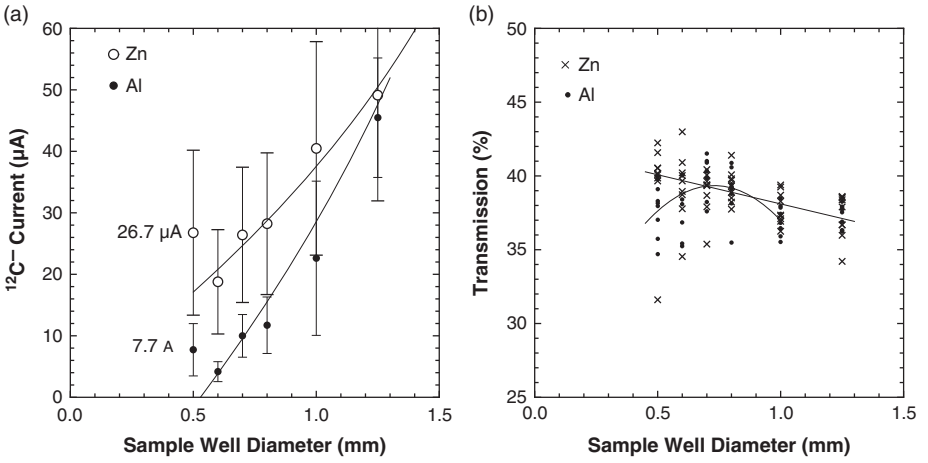

Figure 5 (a) Ion currents from both Zn and Al inserts in three sample holders for each well ⌀ are shown with the standard deviations. At small ⌀, Zn inserts averaged almost 3 times the output of Al inserts. (b) Transmission of the ions was a weak function of well ⌀ with Al inserts giving less C^- transmission than Zn at small ⌀, likely from Coulomb repulsion of an Al_2^- beam.

making competitive Al_2 dimers. Only the 0.5-mm ⌀ wells do not follow the fits, perhaps due to new effects associated with high Cs states driven by greater electron densities in the wells.

Figure 5b shows transmission of the AMS: the fraction of $^{12}C^-$ that is detected as $^{12}C^+$. Transmission increased as the well ⌀ decreased for Zn inserts, expected as the emittance from

https://doi.org/10.1017/RDC.2016.38 Published online by Cambridge University Press

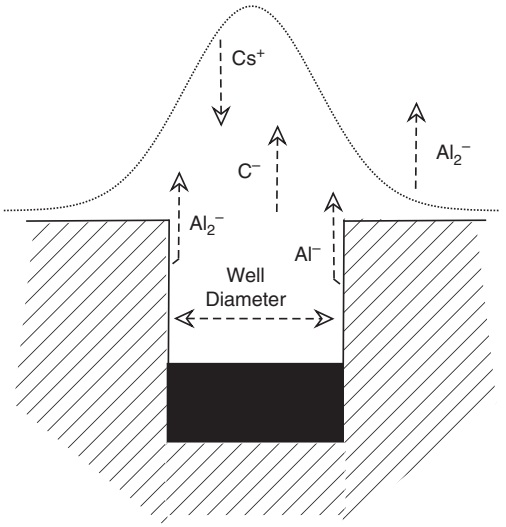

Figure 6 A primary Cs+ beam was integrated across sample wells and onto surrounding Al metal to fit the competition of Al_2^- used in explaining the data in Figure 5a. The Gaussian width of the beam was 1.2 mm.

the sample decreased to better match the ⌀ of the accelerator's gas stripper canal. Transmission for wells in Al inserts decreased at small ⌀, indicating a greater emittance of the C^- beam due to Coulomb repulsion by an increasing Al_2^- and/or Al^- beams. Figures 5a,b show that an increased Al^- and Al_2^- output decreases the C^- current, as proposed above, by competitive ionization of excited Cs states.

DISCUSSION

We confirm the effect discovered by Shanks and Freeman (2015) that sample wells in metals with low EA increase C^- ion currents at small well ⌀ over Al. We used solid metal inserts, while they press powder in a recess into which they drill the sample well. Their approach allows the use of Mn to avoid the dangers of an intense CSIS melting Zn inserts. A 2-mm ⌀ Mn rod (99.5% pure) costs $430 per inch (Goodfellow MN007905, Coraopolis, PA, USA), while a kg of Mn powder of that purity costs only $270 (Goodfellow MN006012). Half-mm wells in both their Fe and our Zn inserts give ~25% more C^- than 1-mm wells in Al. The increase may be due to greater excitation by higher density electrons of Cs to states resonant with C, but is more likely due to increased competition for ionization by Al_2^- from the deeply focused Cs^+ beam hitting the surrounding sample holder. We tried to adjust the MICADAS injection magnet to quantify mass 27 and 54 anions, but were not successful within our time limit. The amount of competitive ionization from Al_2 depends on the primary Cs focus, ~2 mm behind the sample holder surface in our case, and the width of the primary beam, found to be 1.2 mm by the fits in Figure 5a. The "pit casting" done by Shanks and Freeman (2015) show their focus to be 1 mm deeper than the surface, allowing excess Al sputtering. Location of the primary focus at the well entrance (Han et al. 2007) has three advantages: maximal impact of the Cs^+ on the sample for all sample ⌀, erosion of the sample in a ring pattern (keeping the maximum of the ion beam on axis), and minimizing sputtering of the holder material.

Middleton (1994) notes blue plasma forming only after sputter pits form in the samples or if the samples are recessed in wells. He also notes that the secondary sputtered electron (SSE) current

https://doi.org/10.1017/RDC.2016.38 Published online by Cambridge University Press

from the sample cathode reduces as a pit forms. The SSEs in a pit or well arise in a field-free volume but are accelerated away from an unrecessed surface sample, increasing the cathode current. The SSE and wall-reflected electrons reach a density sufficient to excite Cs to high states as the well ⌀ decreases. Taking the well depth to zero in our model is equivalent to mounting the sample flush with the front of the holder. In this configuration, the flows of neutral sputtered Cs and SSE from the sample remain the same, but retention of SSE density within the Cs^0 cloud is missing. The excitement is gone. The sputtered neutral Cs remains in front of the sample, however, available for excitation by laser photoexcitation. We recently tested this by shining a 5-W 450-nm laser "pointer" through the 0.5-mm gap behind the immersion lens of the MICADAS source and obtained a 12% increase in C^-.

We confirm that ionization of sputtered Al and/or Al_2 from the sample holders reduce C^- ion output by competitive ionization. Competitive ionization also explains how Ir and Pt powders in ^{36}Cl samples reduce ^{36}S from the ion source (Vogel 2015) and why Cu sample holders halve C^- output. Further support for the resonant electron transfer theory is obtained from our explanations of several "mysteries" in Middleton's *Negative Ion Cookbook* (Middleton 1989), such as the increased ion output of Al^-, Fe^-, and Cs^-, from narrow-diameter sample wells (Vogel 2015). We further explain why Fe catalyzed C samples provide more C^- than those reduced on Co and Ni, as well as show why Nb is a better metal addition to BeO samples than Ag for AMS (Vogel 2015). Resonant electron transfer continues to explain the operation of CSIS for AMS and offers predictions for improvements.

REFERENCES

Barbier L, Djerad MT, Chéret M. 1986. Collisional ion-pair formation in an excited alkali-metal vapor. *Physical Review A* 34(4):2710.

Bullis RH, Flavin RK. 1964. Research on the collision probabilities of electrons and cesium ions in cesium vapors. Technical Report A-920057-3. United Aircraft Corporation, Research Labs, East Hartford, CT, USA.

Fallon SJ, Guilderson TP, Brown TA. 2007. CAMS/LLNL ion source efficiency revisited. *Nuclear Instruments and Methods in Physics Research B* 259(1):106–10.

Gnaser H. 2008. Isotopic fractionation of sputtered anions: C^- and C_2^-. *Nuclear Instruments and Methods in Physics Research B* 266(1):37–43.

Han BX, Southon JR, Roberts ML, von Reden KF. 2007. Computer simulation of MC-SNICS for performance improvements. *Nuclear Instruments and Methods in Physics Research B* 261(1):589–93.

Kleyn AW, Moutinho AMC. 2001. Negative ion formation in alkali-atom-molecule collisions. *Journal of Physics B* 34(14):R1.

Krishnan U, Stumpf B. 1992. Calculated electron excitation cross sections for excited state-excited state transitions in alkali atoms. *Atomic Data and Nuclear Data Tables* 51(1):151–69.

Lee YT, Mahan BH. 1965. Photosensitized ionization of alkali-metal vapors. *Journal of Chemical Physics* 42:2893–6.

Litherland AE, Paul M, Allen KW, Gove HE. 1987. Fundamentals of accelerator mass spectrometry [and Discussion]. *Philosophical Transactions of the Royal Society of London. Series A, Mathematical and Physical Sciences* 323(1569):5–21.

Marcum SD, Myers JL, Gieske MA, Tackett M, Ganguly BN. 1991. The effect of radiative cascade on electron excitation temperature measurements. *Journal of Applied Physics* 69:27–33.

Middleton R. 1989. *A Negative Ion Cookbook* [unpublished]. Philadelphia: University of Pennsylvania.

Middleton R, Klein J. 1999. Production of metastable negative ions in a cesium sputter source: verification of the existence of N_2^- and CO^-. *Physical Review A* 60(5):3786.

Middleton R, Juenemann D, Klein J. 1994. Isotopic fractionation of negative ions produced by Cs sputtering in a high-intensity source. *Nuclear Instruments and Methods in Physics Research B* 93(1):39–51.

Nalley SJ, Compton RN. 1971. Collisional ionization of cesium by oxygen: the electron affinity of O_2. *Chemical Physics Letters* 9(6):529–33.

Narits AA, Mironchuk ES, Lebedev VS. 2014. Comparative studies of ion-pair formation and resonant quenching processes in collisions of Rydberg atoms with the alkaline-earth atoms. *Journal of Physics B* 47(1):015202.

Norcross DW, Stone PM. 1968. Recombination, radiative energy loss and level populations in nonequilibrium cesium discharges. *Journal of Quantitative Spectroscopy and Radiative Transfer* 8(2):655–84.

https://doi.org/10.1017/RDC.2016.38 Published online by Cambridge University Press

Nørskov JK, Lundqvist BI. 1979. Secondary-ion emission probability in sputtering. *Physical Review B* 19(11):5661.

Shanks RP, Freeman SPHT. 2015. Sputter-pits casting to measure AMS sample consumption. *Nuclear Instruments and Methods in Physics Research B* 361:168–72.

Vogel JS. 2013. Neutral resonant ionization in the high-intensity cesium sputter source. In: Third International Symposium on Negative Ions, Beams and Sources. *AIP Conference Series* 1515:89–98.

Vogel JS. 2015. Anion formation by neutral resonant ionization. *Nuclear Instruments and Methods in Physics Research B* 361:156–62.

Vogel JS. 2016. Anion formation in sputter ion sources by neutral resonant ionization. *Review of Scientific Instruments* 87:02A504.

Vogel JS, Giacomo JA, Dueker SR. 2013. Quantifying absolute carbon isotope ratios by AMS. *Nuclear Instruments and Methods in Physics Research B* 294:340–8.

Vora RB, Turner JE, Compton RN. 1974. Single-electron excitation and transfer in collisions of alkali-metal and oxygen atoms. *Physical Review A* 9(6):2532.

Williams P. 1979. The sputtering process and sputtered ion emission. *Surface Science* 90(2): 588–634.

https://doi.org/10.1017/RDC.2016.38 Published online by Cambridge University Press